J. Fluid Mech. (1974). *vol.* 64, *part* 1, *pp.* 51–63
Printed in Great Britain

Large amplitude convection in porous media

By JOE M. STRAUS

Space Physics Laboratory, Laboratory Operations, The Aerospace Corporation, El Segundo, California 90245

(Received 8 October 1973)

The properties of convective flow driven by an adverse temperature gradient in a fluid-filled porous medium are investigated. The Galerkin technique is used to treat the steady-state two-dimensional problem for Rayleigh numbers as large as ten times the critical value. The flow is found to look very much like ordinary Bénard convection, but the Nusselt number depends much more strongly on the Rayleigh number than in Bénard convection. The stability of the finite amplitude two-dimensional solutions is treated. At a given value of the Rayleigh number, stable two-dimensional flow is possible for a finite band of horizontal wavenumbers as long as the Rayleigh number is small enough. For Rayleigh numbers larger than about 380, however, no two-dimensional solutions are stable. Comparisons with previous theoretical and experimental work are given.

1. Introduction

An understanding of the basic properties of convection in a layer of fluid heated from below is important both from a theoretical and an applied viewpoint. Convective instability is a widespread phenomenon, numerous examples having been noted in geophysical and engineering situations. From a theoretical point of view, convection driven by an adverse temperature gradient is one of the simplest types of hydrodynamic instability, and considerable progress has been made in its study. In particular, since the linear stability problem can be treated rather easily, convective instability has been the subject of many treatments of post-instability flow.

Convection in a porous medium has received less attention than has ordinary Bénard convection. Several experimental studies have been carried out (Schneider 1963; Elder 1967; Combarnous & LeFur 1969; Buretta 1972), but only recently have theoretical analyses of finite amplitude convection in a porous medium been performed (Elder 1967; Palm, Weber & Kvernvold 1972). The present study is motivated by two factors. First, a more complete knowledge of the properties of convection in a porous medium requires that calculations be carried out at Rayleigh numbers larger than those treated by Palm *et al.* These larger Rayleigh numbers are prevalent in naturally occurring convection in porous media, and comparison with experiment requires such calculations. In addition, the equations of motion describing convection in porous media are of lower order than those describing Bénard convection. Therefore, the so-called 'free' boundary conditions are the natural ones in a porous medium. Realistic calculations can thus be carried out rather easily for this type of convection. The fact that simpler equations are involved here than in Bénard convection has been used to great advantage by Busse & Joseph (1972) in an application of the upper-bounding technique to this problem. The present analysis involves a solution of the equations of motion themselves; a comparison of the results with those obtained using the upper-bounding approach is of interest in an assessment of the applicability of results of the upper-bounding technique.

The criterion for the onset of convective flow in a porous medium was predicted theoretically by Lapwood (1948). For Rayleigh numbers above a critical value, laminar flow occurs; Palm *et al.* (1972) have noted that, for Rayleigh numbers somewhat above the critical Rayleigh number, the flow is two-dimensional. The heat flux across a layer of porous material in which convection is occurring has been measured by Combarnous & LeFur (1969); they found that the Nusselt number, the ratio of the actual heat transport to that which would occur in the absence of convection, increases continuously as a function of Rayleigh number up to a value of the Rayleigh number approximately seven times the critical one; at this point a change in the slope of the heat-transport curve occurs. This behaviour is similar to that noted by Malkus (1954) to occur in Bénard convection. As shown by Busse (1967), this phenomenon is thought to be due to the instability of the boundary layers which form at supercritical Rayleigh numbers and is associated with a transition to a regime in which no stable two-dimensional convective flow is possible (Busse & Whitehead 1971). If the analogy between Bénard convection and convection in a porous medium holds, the transition noted by Combarnous & LeFur (1969) should correspond to the transition to a regime in which only three-dimensional flow is possible.

The present analysis is divided into two parts. First, the equations describing steady convection in a porous medium are developed, and the two-dimensional problem is solved numerically using the Galerkin technique for Rayleigh numbers up to ten times the critical value. Properties of this steady flow are discussed, particularly those associated with the heat flux and its variation with wavenumber. The second part deals with the stability of the two-dimensional solutions to infinitesimal perturbations. Two distinct types of perturbations are treated, and separate analyses are given for each.

2. Formulation of the problem

Consider a horizontally infinite layer of porous material saturated with fluid. The layer has horizontal boundaries at $z = 0$ and d on which the temperature T is specified:

$$T(0) = T_0, \quad T(d) = T_0 + \Delta T.$$

The equations of motion admit the motionless basic state

$$T_1 = T_0 + (\Delta T/d)\, z.$$

The stability of this state will be examined. The non-dimensional Boussinesq equations of motion governing an arbitrary perturbation are

$$B(\partial \mathbf{u}/\partial t+\mathbf{u}.\nabla \mathbf{u}) = -\nabla p+R\theta\hat{\mathbf{z}}-\mathbf{u}, \tag{1}$$

$$\partial\theta/\partial t+\mathbf{u}.\nabla\theta = \nabla^2\theta+w, \tag{2}$$

$$\nabla.\mathbf{u} = 0. \tag{3}$$

Here $\mathbf{u}$ is the perturbation velocity, p is the perturbation pressure, θ is the temperature perturbation $(T-T_1)$, $\hat{\mathbf{z}}$ is the vertical unit vector and $w = \mathbf{u}.\hat{\mathbf{z}}$. The velocity $\mathbf{u}$ is an average over the microscale of the porous medium. These macroscopic equations are valid as long as the pore size of the medium is smaller than any scale size of the flow. At very large Rayleigh numbers, the applicability of these equations may break down because of the formation of boundary layers near the top and bottom boundaries. Non-dimensionalization has been accomplished by using d as the length scale, d^2/κ as the time scale, ΔT as the temperature scale and κ/d as the velocity scale. The two parameters R and B are, respectively, the Rayleigh number and a Prandtl number:

$$R = \gamma g K d\Delta T/\nu\kappa, \quad B = K\kappa/d^2\nu,$$

where γ is the thermal expansion coefficient, g is the acceleration due to gravity, K is the permeability of the porous medium, ν is the kinematic viscosity of the fluid, and κ is a thermal diffusivity defined as the thermal conductivity of the porous medium divided by the specific heat and density of the fluid (Katto & Masuoka 1967). Note that the equations are almost identical to those of Bénard convection; the replacement of $\nabla^2\mathbf{u}$ by $-\mathbf{u}$ allows only two conditions to be imposed on the boundaries. These will be taken to be

$$w = \theta = 0 \quad \text{at} \quad z = 0, 1. \tag{4}$$

This corresponds to boundaries on which the temperature is fixed and through which no flow occurs. Now, for most situations of interest, $B \ll 1$; we shall therefore carry out the analysis in the limit $B \to 0$. This is particularly appropriate in that Darcy's law, the equation of motion for flow in a porous medium, has no inertial term in it. As Muskat (1937) has pointed out, the absence of the inertial term is due to the comparative unimportance of the acceleration forces as compared with the internal friction resistances in a fluid-bearing medium. In our notation, this situation is explicitly taken into account through the use of the limit $B \to 0$.

In order to develop the equations to be solved, we shall introduce new notation. Since both the vertical component of vorticity and the divergence of the velocity vanish, we may write

$$\mathbf{u} = \boldsymbol{\delta}\phi, \quad \text{where} \quad \boldsymbol{\delta} = (\partial_{xz}, \partial_{yz}, -\nabla_1^2), \quad \nabla_1^2 = (\partial_{xx}+\partial_{yy}).$$

The equations of motion may then be written as

$$-R\theta = \nabla^2\phi, \tag{5}$$

$$\partial\theta/\partial t+\boldsymbol{\delta}\phi.\nabla\theta = \nabla^2\theta-\nabla_1^2\phi, \tag{6}$$

subject to the boundary conditions $\nabla_1^2\phi = \theta = 0$ at $z = 0, 1$.

The linear stability problem is given by

$$R\theta = -\nabla^2\phi, \quad \nabla^2\theta = \nabla_1^2\phi + \partial\theta/\partial t.$$

The principle of exchange of stabilities can be shown to hold, and the condition for the onset of instability can be written as

$$R > R_c = (\alpha^2+\pi^2)^2/\alpha^2,$$

where we have assumed that θ and ϕ are of the form

$$\phi = f(x,y)\,\phi_1(z), \quad \theta = f(x,y)\,\theta_1(z),$$

where $\nabla_1^2 f = -\alpha^2 f$ and ϕ_1 and θ_1 satisfy the prescribed boundary conditions on $z = 0, 1$. R_c takes on the minimum value $4\pi^2$ when $\alpha = \pi$.

3. The finite amplitude steady solutions

In this section we shall solve the two-dimensional steady problem using the Galerkin technique, first used in the study of thermal convection by Veronis (1966).

Assuming that θ and ϕ are periodic in the horizontal, expand θ in a Fourier series satisfying the boundary conditions:

$$\theta = \sum_{\lambda,\nu} a_{\lambda\nu}\, e^{i\lambda\alpha x}\sin\nu\pi z,$$

where $-\infty < \lambda < \infty$, $1 \leqslant \nu < \infty$ and $a_{\lambda\nu} = a^*_{-\lambda\nu}$. A similar expansion for ϕ may be written down:

$$\phi = \sum_{\lambda,\nu} \frac{R\, a_{\lambda\nu}\, e^{i\lambda\alpha x}\sin\nu\pi z}{(\lambda\alpha)^2+(\nu\pi)^2}, \tag{7}$$

where (5) has been used. We then substitute these expressions into (6), multiply by $e^{-i\rho\alpha x}\sin\eta\pi z$ and integrate over the layer. We obtain an infinite set of coupled first-order ordinary differential equations for the $a_{\lambda\nu}$. It is necessary to truncate these series solutions to obtain a finite set of equations. This is accomplished by restricting λ and ν such that $|\lambda|+\nu \leqslant N$, where N is a positive integer. This method of truncation has been discussed in detail by Veronis (1966). Values of N as large as 16 were used in the present study. The particular method for solving the equations and the convergence criterion used are described by Straus (1972). In short, the convergence was measured by the convergence of the Nusselt number

$$Nu = 1+\pi\sum_{\nu}\nu a_{0\nu}$$

as a function of N. It was found that $N = 16$ was sufficient to compute accurately the properties of convection for Rayleigh numbers as large as 400. The values of the Nusselt number should be accurate to within 1 %.

The calculations were carried out in the following manner. For a given value of R, the Fourier coefficients $a_{\lambda\nu}$ are functions of N as well as of the horizontal wavenumber α. For example, if the series is truncated at $N = 2$, we may derive the following expression for Nu:

$$Nu = 3-\frac{2}{R}(\alpha^2+\pi^2)^2/\alpha^2. \tag{8}$$

α^2/π^2	Nu (N = 2)	Nu (N = 8)	Nu (N = 10)
1·25	2·600	3·874	3·888
1·50	2·589	3·926	3·928
1·75	2·574	3·948	3·950
2·0	2·556	3·969	3·981
2·5	2·517	3·993	4·010
3·0	2·474	4·001	4·026
3·5	2·430	4·003	4·028
4·0	2·384	3·986	4·022
5·0	2·290	3·906	3·932

TABLE 1. Nu as a function of N and α for R = 200.

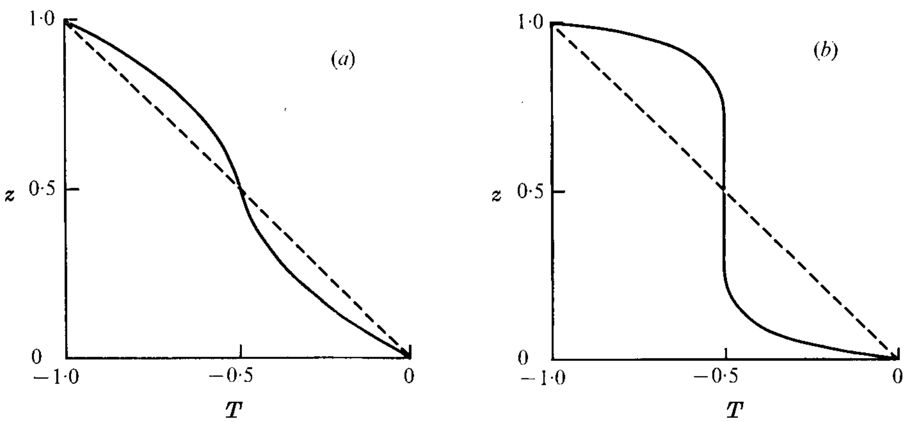

FIGURE 1. The horizontally averaged temperature fields for finite amplitude convection in a porous medium. (a) $R = 60$, $\alpha = \pi$. (b) $R = 400$, $\alpha = 2{\cdot}9\pi$.

This is the same expression as may be derived using perturbation expansion methods such as that used by Palm *et al.* (1972). However, it is only accurate for $R \lesssim 2R_c$. Both the Nusselt number and the wavenumber α needed to maximize it are given accurately at larger values of R only by the results of computations at larger values of N. An example of this is given in table 1. The values of Nu given by the $N = 2$ calculation are clearly too low; in addition, the wavenumber required to maximize Nu is larger than the value $\alpha = \pi$ predicted by the $N = 2$ result, although the Nusselt number varies only weakly with α.

As is well known in studies of Bénard convection, as the Rayleigh number is increased above R_c, boundary layers begin to form at the top and bottom boundaries. This allows the interior of the fluid to approach isothermality, while the heat flux across the boundaries is increased owing to the large temperature gradient there. This boundary layering also occurs in convection in porous media. Figure 1 shows the horizontally averaged temperature field as a function of z. The situations for two values of the Rayleigh number are shown: $R = 60$ with $\alpha = \pi$ and $R = 400$ with $\alpha = 2{\cdot}9\pi$. It is clear that the boundary layers become much stronger as R increases. In fact, for large values of R the

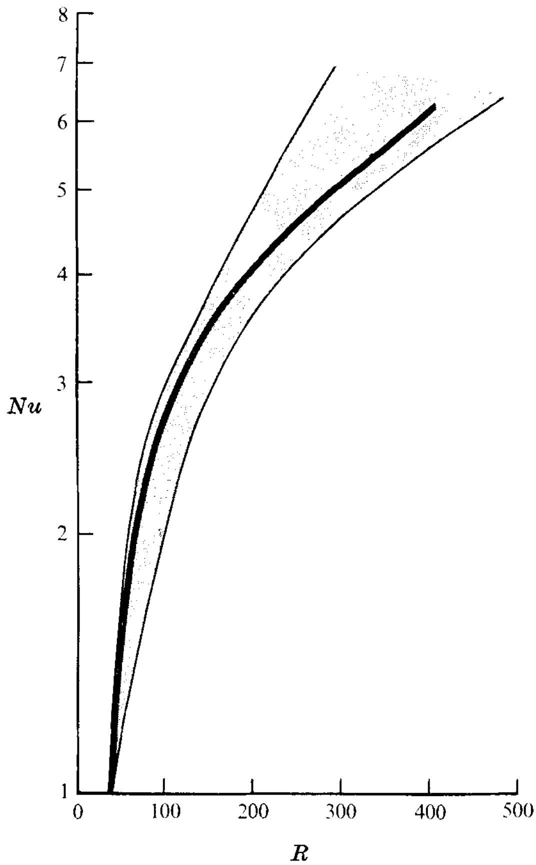

FIGURE 2. The Nusselt number as a function of Rayleigh number: the heavy curve represents results of the present analysis; the shaded area indicates the range of experimental measurements by Schneider (1963), Elder (1967), Combarnous & LeFur (1969) and Buretta (1972).

boundary-layer thickness is thought to become comparable with the pore size, and the applicability of the equations of motion as formulated here probably breaks down. Another effect should be pointed out here. The wavenumbers for which figure 1 was drawn are approximately those which maximize the heat flux at the given values of R. A wavenumber considerably different from that which maximizes the heat flux leads to a horizontally averaged temperature profile which shows much less boundary-layer structure. This behaviour is in agreement with the fact that a large convective heat flux is associated with strong boundary layers.

In figure 2 is shown the variation of Nusselt number with Rayleigh number as calculated in this analysis. The Nusselt number is the maximum value which occurs, as a function of wavenumber, at each value of R. Also shown is the range of experimental results as given by the investigators mentioned earlier. For large Rayleigh numbers, the present numerical results appear to lie in the lower part of the range of experimental values. Since there is quite a bit of scatter in the experimental measurements, and since each measurement has perhaps a 10 % uncertainty, this fact is not thought to be of significance.

4. Stability of the finite amplitude solutions

In this section the stability of the finite amplitude two-dimensional solutions described earlier will be discussed. The equations governing arbitrary three-dimensional infinitesimal perturbations $\tilde{\theta}$ and $\tilde{\phi}$ may be written as

$$R\tilde{\theta} = -\nabla^2\tilde{\phi}, \tag{9}$$

$$\partial\tilde{\theta}/\partial t = -\boldsymbol{\delta}\phi . \nabla\tilde{\theta} - \boldsymbol{\delta}\tilde{\phi} . \nabla\theta + \nabla^2\tilde{\theta} - \nabla_1^2\tilde{\phi}, \tag{10}$$

where $\tilde{\phi}$ and $\tilde{\theta}$ must satisfy the same boundary conditions at $z = 0, 1$ as do ϕ and θ. We are interested in determining whether there exist solutions $\tilde{\phi}$ and $\tilde{\theta}$ which, at given values of R and α, grow in time. Specifically, if $\partial\tilde{\theta}/\partial t$ is positive for any $\tilde{\theta}$, the steady two-dimensional solution is unstable; if not, it is stable.

As Busse (1967) has pointed out for the case of Bénard convection, since the stability equations (9) and (10) are linear differential equations with constant coefficients with respect to time and the y co-ordinate, the solution can be written as the sum of solutions which depend exponentially on the three spatial co-ordinates, multiplied by a function of x with the same periodicity as the stationary solution. We shall write the perturbation in temperature as

$$\tilde{\theta} = \sum_{\lambda,\nu} \tilde{a}_{\lambda\nu}\, e^{i\lambda\alpha x} \sin \nu\pi z\, e^{i(dx+by)}\, e^{pt}. \tag{11}$$

Equation (9) then yields the following form for $\tilde{\phi}$:

$$\tilde{\phi} = \sum_{\lambda,\nu} \frac{R\, \tilde{a}_{\lambda\nu}\, e^{i\lambda\alpha x} \sin \nu\pi z\, e^{i(dx+by)}\, e^{pt}}{(\lambda\alpha + d)^2 + b^2 + (\pi\nu)^2}. \tag{12}$$

A set of equations governing the coefficients $\tilde{a}_{\lambda\nu}$ may then be developed in the same manner as that used in the analysis of the steady equations. The growth rate p governs the stability of the steady solutions $\tilde{\theta}$ and $\tilde{\phi}$: if p has a positive real part, the steady flow is unstable; otherwise, it is stable.

There are two types of disturbances which appear to be most important when R is near R_c. For $\alpha > \pi$, disturbances at right angles to the original rolls are most destablizing. For $\alpha < \pi$ and R smaller than some value, the steady flow becomes unstable to a disturbance oriented at a small angle with respect to the original roll. The expansion procedure discussed above may be used to treat both types of instability. However, the second type of instability may be more accurately analysed using a method developed by Lortz (1968) for Bénard convection. Since the disturbance growth rate is dependent on the value of the y component of the disturbance wave vector, a small quantity in the case of disturbances almost aligned with the steady roll, the stability boundary may be described using a singular perturbation expansion. This analysis was applied to Bénard convection by Straus (1972) and will only be outlined here.

The equations for steady two-dimensional motion may be written as

$$\boldsymbol{\delta}\phi\,.\,\nabla\nabla^2\phi-\nabla^4\phi-R\nabla_1^2\phi = 0, \tag{13}$$

where ϕ satisfies the boundary conditions $\phi = \partial^2\phi/\partial z^2 = 0$ at $z = 0, 1$, and $\phi = \phi(x,z)$. Perturbing the solutions of this equation with small disturbances $\tilde{\phi}(x,y,z)$, we write

$$\partial(\nabla^2\tilde{\phi})/\partial t+\boldsymbol{\delta}\tilde{\phi}\,.\,\nabla\nabla^2\phi+\boldsymbol{\delta}\phi\,.\,\nabla\nabla^2\tilde{\phi}-\nabla^4\tilde{\phi}-R\nabla_1^2\tilde{\phi} = 0. \tag{14}$$

Since we are interested in disturbances which are almost aligned with the rolls which are solutions of (13), we write

$$\tilde{\phi} = f(x,z)\,e^{\sigma t}\,e^{imy},$$

where m is small, and expand

$$f = f_0+m^2f_1+\ldots,\quad \sigma = \sigma_0+m^2\sigma_1+\ldots.$$

Using this formulation in (14), we may derive the following equation for f_0:

$$\partial_x\partial_z f_0\partial_x\nabla^2\phi-\partial_{xx}f_0\partial_z\nabla^2\phi+\partial_x\partial_z\phi\partial_x\nabla^2f_0-\partial_{xx}\phi\partial_z\nabla^2f_0-R\partial_{xx}f_0-\nabla^4f_0 = 0. \tag{15}$$

A solution with $\sigma_0 = 0$ is $f_0 = \partial_x\phi$. Similarly the $O(m^2)$ equation is

$$\begin{aligned}&-\sigma_1\nabla^2f_0-f_0\partial_z\nabla^2\phi+\partial_x\partial_z\phi\partial_x f_0-\partial_{xx}\phi\partial_z f_0-Rf_0-2\nabla^2f_0\\&\quad= \partial_x\partial_z f_1\partial_x\nabla^2\phi-\partial_{xx}f_1\partial_z\nabla^2\phi+\partial_x\partial_z\phi\partial_x\nabla^2f_1-\partial_{xx}\phi\partial_z\nabla^2f_1-R\partial_{xx}f_1-\nabla^4f_1.\end{aligned} \tag{16}$$

This equation has a solution if, and only if,

$$\begin{aligned}\sigma_1\int_0^1\int_0^{2\pi/\alpha}\Psi\nabla^2f_0\,dx\,dz = \int_0^1\int_0^{2\pi/\alpha}&\Psi[-f_0\,\partial_z\nabla^2\phi+\partial_x\partial_z\phi\,\partial_x f_0\\&-\partial_{xx}\phi\,\partial_z f_0-Rf_0-2\nabla^2f_0]\,dx\,dz,\end{aligned}$$

where Ψ is the solution to the problem that is adjoint to (15):

$$\begin{aligned}&\partial_x\partial_z[\Psi\,\partial_x\nabla^2\phi]-\partial_{xx}[\Psi\,\partial_z\nabla^2\phi]-\partial_x\nabla^2[\Psi\,\partial_z\partial_x\phi]\\&\qquad+\partial_z\nabla^2[\Psi\,\partial_{xx}\phi]-R\,\partial_{xx}\Psi-\nabla^4\Psi = 0.\end{aligned}$$

A solution to this is $\Psi = \partial_x\phi$. Thus, the solvability condition may be written as

$$\sigma_1\int_0^1\int_0^{2\pi/\alpha}\frac{\partial\phi}{\partial x}\nabla^2\frac{\partial\phi}{\partial x}\,dx\,dz = \int_0^1\int_0^{2\pi/\alpha}\frac{\partial\phi}{\partial x}\left[-\frac{\partial\phi}{\partial x}\frac{\partial}{\partial z}\nabla^2\phi-R\frac{\partial\phi}{\partial x}-2\nabla^2\frac{\partial\phi}{\partial x}\right]dx\,dz. \tag{17}$$

Since the integral on the left side of (17) is negative, the flow described by ϕ is unstable if

$$\int_0^1\int_0^{2\pi/\alpha}\frac{\partial\phi}{\partial x}\left[\frac{\partial\phi}{\partial x}\frac{\partial}{\partial z}\nabla^2\phi+R\frac{\partial\phi}{\partial x}+2\nabla^2\frac{\partial\phi}{\partial x}\right]dx\,dz > 0. \tag{18}$$

Thus, once ϕ is known, the stability of the flow to a disturbance aligned at a small angle to that described by ϕ may be examined. We shall use the expression for ϕ given by (7) where the coefficients $a_{\lambda\nu}$ have been determined numerically as described in the previous section. One must recognize that this analysis assumes that there is no oscillatory instability. This unlikely situation cannot be ruled out using this method, but application of the more general stability analysis, discussed below, indicates that all stability boundaries are determined by instabilities which set in as monotonically growing disturbances. It is of interest to note that a useful stability criterion for R near R_c can be derived from the relation (18). If we take $\phi = \epsilon \cos \alpha x \sin \pi z$, where ϵ is a small but finite amplitude, and substitute this into (18), keeping only terms of lowest order in ϵ, we find the criterion for instability:

$$R > 2(\alpha^2 + \pi^2).$$

Now, if $R = (\alpha^2 + \pi^2)^2/\alpha^2$, we find that this requires

$$\alpha < \pi.$$

The inclusion of higher-order terms modifies this result. The results of this calculation are shown in figure 4 as the stability boundary for $\alpha < \pi$ where R is less than a value determined by the intersection of this stability boundary with that due to disturbances at right angles to the steady rolls. The latter disturbances are discussed below.

The stability of the steady flow with respect to disturbances at larger angles can best be treated using the expansions (11) and (12). The series is truncated by including only those $\tilde{a}_{\lambda\nu}$ such that $|\lambda| + \nu \leqslant N+1$, where N is the same N as that used to truncate the set of steady equations. In this way, all $a_{\lambda\nu}$ included in the corresponding steady calculation are included in the stability analysis. The stability equations are eigenvalue equations for p, and the problem is to determine, at given values of R and α, whether it is possible that there is a value of p with a positive real part. In order to answer this question, we have used the same technique as was used by Busse (1967) and, subsequently, by Straus (1972). Since the matrices involved can be as large as 91×91, we have calculated only the eigenvalue with the smallest absolute value. This is reasonable since it is known that, near R_c, there is a region of stable two-dimensional solutions, at least for $\alpha > \pi$. Thus, at a given value of $R > R_c$, instability will be indicated by the eigenvalue with the largest real part passing through zero from negative to positive. An iterative procedure was used to calculate the eigenvalue with the smallest absolute value. The iterative method converges only if the eigenvalue with the smallest absolute value is real. Since convergence was always attained, it is reasonable to conclude that no oscillatory instability is involved.

Even using this iterative approach, the stability problem is a formidable one. Both d and b must be varied at each value of R and α analysed. Fortunately, the maximum growth rate always occurred when $d = 0$; thus, some decrease in the number of computations required resulted. The value of b which leads to a maximum value of p, at a given value of R, varies continuously as the value of the wavenumber α of the finite amplitude roll solution varies: the quantity $\alpha^2 + b^2$ remains fairly constant (in comparison with the range of values over which α and b vary individually). Figure 3 shows the relevant growth rates for $R \leqslant 400$. In general, the growth rate is positive outside a band of wavenumbers; only within this limited band are the two-dimensional solutions stable. This band, which includes only the wavenumber $\alpha = \pi$ at $R = R_c$, increases in width

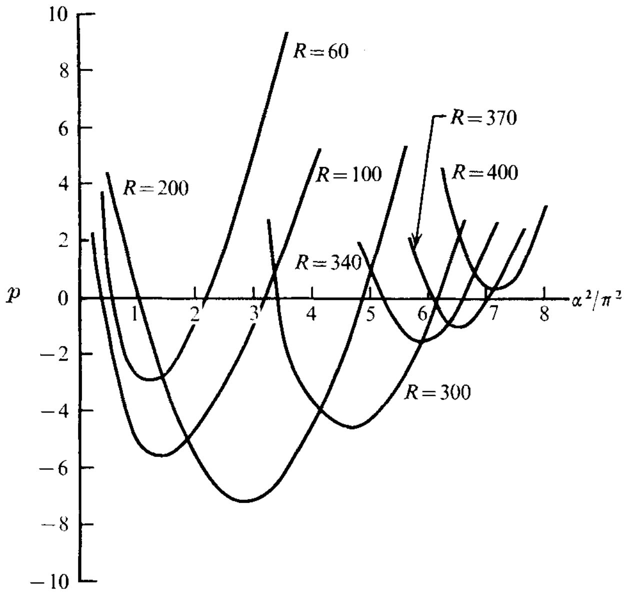

FIGURE 3. The growth rate of the most critical disturbance as a function of α at given values of R.

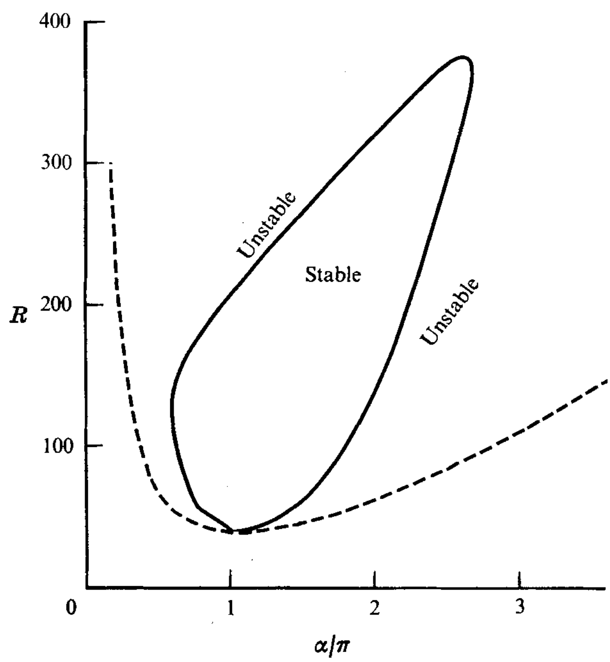

FIGURE 4. The region of stable two-dimensional solutions: above dashed line, instability of the basic motionless state occurs; only within the closed region are finite amplitude two-dimensional solutions stable.

to a maximum at $R \sim 150$. It then decreases until, above a Rayleigh number of 380 ± 5, no two-dimensional rolls are stable.

Figure 4 shows the stability boundary for both types of disturbances discussed here. For low values of R and $\alpha < \pi$, disturbances almost aligned with the original roll limit the region of stable rolls most strongly. However, for values of R greater than about 58 when $\alpha < \pi$, and for all values of R when $\alpha > \pi$, disturbances at larger angles predominate. The vanishing of the region of stable rolls for Rayleigh numbers larger than 380 ± 5 indicates that a three-dimensional flow must exist for larger Rayleigh numbers.

5. Discussion

The results of the preceding analysis and comparisons with other relevant work will be discussed here. The equations of motion describing flow in a porous medium are considerably simpler than those describing the flow of a pure fluid. The physics describing convective flows in the two situations are, however, the same, at least in Bénard convection in a large Prandtl number fluid. Thus, the problem of convection in a porous medium is one which may be treated with comparative ease as a model problem in the study of post-instability flow. The present treatment of finite amplitude convection in a porous medium has been largely a numerical one. The Galerkin technique has been used to determine the properties of steady convection in a porous medium at Rayleigh numbers as large as ten times the critical value. The Nusselt number and the horizontally averaged temperature field have been described as functions of Rayleigh number and horizontal wavenumber. The stability of the steady flow to three-dimensional perturbations has been examined using a matrix iterative technique.

The quantity most often measured in convection experiments is the Nusselt number. A comparison of the results of the present analysis with the experimental results of Combarnous & LeFur (1969), Buretta (1972), Elder (1967) and Schneider (1963) shows generally good agreement. There is considerable scatter in the experimental points, and the behaviour of the Nusselt number as a function of Rayleigh number derived here lies within the range of the experimental results.

Theoretical treatments of convection in porous media have been of several types. Elder (1967) used a finite difference method to treat porous-medium convection in a square box for values of $R \leqslant 100$. His results are approximately 2 % lower than ours at $R = 100$; this is probably because the wavenumber in his calculations was determined by the horizontal extent of his model. A square box allows only flows of larger wavenumbers than the value $\alpha \sim 1{\cdot}2\pi$, found to maximize the heat flux at $R = 100$ in the present analysis. Since the heat flux is maximum when $\alpha = 1{\cdot}2\pi$, a lower value is expected at all other wavenumbers. Palm *et al.* (1972) applied Kuo's (1961) expansion technique to this problem. Their results lie somewhat above the results of the present analysis; the reason for this is not known, but may lie in the different ordering schemes used in their analysis and the present one. In any case, the difference in the Nusselt numbers is no larger than the spread in the experimental results.

The problem of convection in a porous medium has also been the subject of treatments using the upper-bounding method introduced by Howard (1963) in an analysis of Bénard convection. Busse & Joseph (1972) applied the upper-bounding technique to porous-medium convection in a fluid with an arbitrary value of B. This approach appears to be too general to yield values of the Nusselt number close to those of experiment, as the upper bound on the Nusselt number increases with R much too strongly, leading to a behaviour $Nu \sim e^R$ as $R \to \infty$. A more restrictive problem has recently been treated by Gupta & Joseph (1973), who applied the upper-bounding technique in the case $B \to 0$. Their results are much more realistic: their numerical calculations lead to a Nusselt number lying along the upper boundary of the range of experimental results given in figure 2. However, their results are still somewhat larger than those given by the present calculations. At $R = 100$, the Nusselt number given by Gupta & Joseph is already some 5 % higher than that found here.

Finally, the stability analysis indicates that, for a given value of R, there is a range of horizontal wavenumbers for which stable two-dimensional convection exists, if R is small enough. For values of $R \gtrsim 380$, there are no stable two-dimensional solutions, and three-dimensional motion occurs for all values of the wavenumber. This value of R is to be compared with the value 280, at which the experiments of Combarnous & LeFur (1969) indicate that there is a change of slope in the dependence of the heat flux on the Rayleigh number. This is a phenomenon similar to that observed by Malkus (1954) to occur in Bénard convection and later shown by Busse (1967) to be associated with the instability of the boundary layers at the top and bottom boundaries of the convecting layer. The larger value of R found numerically is to be expected; it represents an upper limit on this second critical Rayleigh number because finite amplitude instability may limit the region of two-dimensional solutions more strongly than does instability due to infinitesimal perturbations.

It is a pleasure to acknowledge helpful discussions with Professor F. H. Busse. This work was supported by U.S. Air Force Space and Missile Systems Organization (SAMSO) Contract F04701-72-0073.

REFERENCES

BURETTA, R. 1972 Ph.D. dissertation, University of Minnesota.
BUSSE, F. H. 1967 *J. Math. & Phys.* **46**, 140.
BUSSE, F. H. & JOSEPH, D. D. 1972 *J. Fluid Mech.* **54**, 521.
BUSSE, F. H. & WHITEHEAD, J. A. 1971 *J. Fluid Mech.* **47**, 305.
COMBARNOUS, M. & LEFUR, B. 1969 *Comptes Rendus*, **269**, 1009.
ELDER, J. W. 1967 *J. Fluid Mech.* **27**, 29.
GUPTA, V. P. & JOSEPH, D. D. 1973 *J. Fluid Mech.* **57**, 491.
HOWARD, L. N. 1963 *J. Fluid. Mech.* **17**, 405.
KATTO, Y. & MASUOKA, T. 1967 *Int. J. Heat & Mass Transfer*, **10**, 297.
KUO, H. L. 1961 *J. Fluid Mech.* **10**, 611.
LAPWOOD, E. R. 1948 *Proc. Camb. Phil. Soc.* **44**, 508.
LORTZ, D. 1968 *Z. angew. Math. Phys.* **19**, 682.

MALKUS, W. V. R. 1954 *Proc. Roy. Soc.* A **225**, 185.

MUSKAT, M. 1937 *The Flow of Homogeneous Fluids Through Porous Media*, pp. 121–146. J. W. Edwards.

PALM, E., WEBER, J. E. & KVERNVOLD, O. 1972 *J. Fluid Mech.* **54**, 153.

SCHNEIDER, K. J. 1963 *11th Int. Cong. Refrigeration (Munich)*, paper 11·4.

STRAUS, J. M. 1972 *J. Fluid Mech.* **56**, 353.

VERONIS, G. 1966 *J. Fluid Mech.* **26**, 49.